JOURNAL OF CATALYSIS **166,** 284–293 (1997)
ARTICLE NO. CA971508

# Effects of Pt Precursors on Hydrodechlorination of Carbon Tetrachloride over $Pt/Al_2O_3$

Hyun Chul Choi, Sun Hee Choi, Jae Sung Lee, Kyung Hee Lee,[1] and Young Gul Kim

*Department of Chemical Engineering, Pohang University of Science and Technology(POSTECH), San 31 Hyoja-dong, Pohang, 790-784 Korea*

Received June 5, 1996; revised September 26, 1996; accepted October 30, 1996

**Hydrodechlorination of carbon tetrachloride ($CCl_4$) has been studied over 1% $Pt/Al_2O_3$ prepared from various Pt precursors. The $Pt/Al_2O_3$ catalyst prepared from Pt(II) precursors showed stable, high conversion of $CCl_4$ above 99% and selectivity of $CHCl_3$ above 78% at the reaction temperature of 393 K, $H_2/CCl_4$ mole ratio of 9 and weight hourly space velocity of 9000 liters/kg/h. Relative to fresh catalyst, amounts of carbon and chlorine increased in catalysts which had been used for the reaction and, in particular, when the catalysts showed deactivation. Used catalyst showed a decrease in the amount of $H_2$ chemisorption and the decrease was greater for catalysts prepared from Pt(IV) precursors than those from Pt(II) precursors. The catalyst prepared by $Pt(NH_3)_2(NO_2)_2$ indicated a retarded coke formation compared to that from $H_2PtCl_6$. From temperature-programmed reduction, temperature-programmed oxidation, and X-ray absorption fine structure measurements, it was concluded that the difference between the catalysts prepared from Pt(II) and Pt(IV) precursors was due to the different oxidation states of Pt.** 

## INTRODUCTION

Catalytic hydrodechlorination of carbon tetrachloride (CTC) is a promising method to dispose of CTC which has been classified as a material of Group IV among ozone depleting chlorofluorocarbons (CFCs) and whose use has been banned in developed countries from 1996. Noble metals are preferred catalysts which convert CTC into useful products such as $CHCl_3$ and $CH_2Cl_2$ at mild temperatures of 380–480 K (1, 2). Despite the intensive research since the 1990s, especially in industrial laboratories, reported catalysts have drawbacks in selectivity and/or stability (3–8).

In our previous studies (9, 10), we studied the effects of various supports ($\gamma$-$Al_2O_3$, $SiO_2$, MgO, $TiO_2$, $SiO_2$–$Al_2O_3$, $ZrO_2$, NaY) in Pt catalyzed hydrodechlorination of CTC. For 1 wt% Pt loading accomplished by impregnation with a $H_2PtCl_6$ solution, MgO was found to be the most selective support toward formation of $CHCl_3$ and the most stable support against the catalyst deactivation. The optimum reaction conditions to obtain stable and high conversions of CTC above 90% were a reaction temperature of 413 K, $H_2$/CTC mole ratio of 9 and weight hourly space velocity (WHSV) of 9000 liters CTC/kg catalyst/h. From the X-ray photoelectron spectroscopy (XPS) and X-ray absorption fine structure (XAFS) measurements, the active phase of Pt during hydrodechlorination appeared to be a surface Pt(II) species with Cl ligands, while the bulk remained as Pt metal. An alumina-supported Pt catalyst showed high activity and good selectivity toward formation of $CHCl_3$. Yet it gradually lost its activity during the course of the reaction. The main cause of this deactivation was found to be the coke deposition on the catalyst. In the present paper, effects of Pt precursors such as $H_2PtCl_6$, $K_2PtCl_6$, $(NH_4)_2PtCl_6$, $Pt(NH_3)_4Cl_2$, $Pt(NH_3)_2(NO_2)_2$, and $Pt(NH_3)_4(NO_3)_3$ have been studied in the hydrodechlorination of CTC over 1% $Pt/Al_2O_3$ catalyst. Various analytical methods (XPS, $H_2$ chemisorption, XAFS, temperature-programmed reduction (TPR), temperature-programmed oxidation (TPO)) were employed in order to elucidate the correlation between the catalyst precursor and catalytic properties of 1% $Pt/Al_2O_3$ such as the selectivity toward formation of $CHCl_3$ and catalyst deactivation.

## EXPERIMENTAL

$Pt(NH_3)_2(NO_2)_2$ (Aldrich), $Pt(NH_3)_4Cl_2 \cdot xH_2O$ (Aldrich), $Pt(NH_3)_4(NO_3)_2$ (Korea Engelhard), $H_2PtCl_6 \cdot xH_2O$ (Aldrich), $K_2PtCl_6$ (Aldrich), and $(NH_4)_2PtCl_6$ (Aldrich) were used as Pt precursors to the catalysts. $\gamma$-$Al_2O_3$ (Strem, surface area, $95 \pm 2$ m$^2$ g$^{-1}$, pore volume, $0.5 \pm 0.05$ ml g$^{-1}$) was impregnated with an aqueous Pt solution. After drying for 24 h at 383 K, the samples were calcined in oxygen flow (>99.99%) for 2 h at increasing temperatures up to 573 K (heating rate, 5 K min$^{-1}$) and then reduced in hydrogen flow (>99.99%) for 2 h again at increasing temperatures up to 573 K (heating rate, 5 K min$^{-1}$). The platinum loading was 1 wt% (as metal), and the content of Pt in the catalyst was confirmed to be $1.0 \pm 0.02$ wt% in a postanalysis by inductively coupled plasma-atomic emission spectroscopy.

[1] To whom correspondence should be addressed.



0021-9517/97 $25.00

The chemisorption of hydrogen was carried out in a conventional volumetric adsorption apparatus at room temperature (RT) in the pressure range of 10–70 kPa. The sample was first reduced *in situ* under hydrogen flow at 573 K for 2 h, then evacuated to $1 \times 10^{-5}$ Pa at 673 K for 1 h. The sample was cooled to RT and the first $H_2$ chemisorption isotherm was taken. The sample was then evacuated to $1 \times 10^{-5}$ Pa at RT, and the second isotherm was taken. The linear part of two isotherms was extrapolated to zero pressure. The amount of chemisorbed $H_2$ was the difference of two isotherms at zero pressure. The particle size $d_p$ of Pt was estimated from the $H_2$ chemisorption data assuming spherical Pt particles (11, 12). The size of the metallic particles was also checked by high resolution transmission electron microscopy (TEM) using a JEOL JEM-400FX microscope.

The $N_2$ BET surface area $S_g$ was measured in the volumetric adsorption apparatus (Micrometrics, Accusorb 2100E) at liquid nitrogen temperature. XPS spectra were recorded using a PHI 5400 ESCA spectrometer employing Mg K$\alpha$ source ($h\nu = 1253.6$ eV) and an energy shift due to charging effect was carefully corrected with a carbon peak at 284.6 eV as a standard.

TPR measurements were performed with a 5% $H_2$/95% $N_2$ gas mixture for calcined samples following the pretreatment with He gas at 773 K for 2 h. The temperature range was 373 K to 773 K with a ramp of 10 K $min^{-1}$. The $H_2$ consumption was monitored by a thermal conductivity detector (TCD). A molecular sieve trap was placed after the catalyst and in front of the TCD in order to trap out water before detection. TPO experiments were carried out with a 1% $O_2$/99% He gas mixture for used and deactivated catalysts pretreated with He gas at 773 K for 2 h. The temperature range was from 373 K to 773 K with a ramp of 10 K $min^{-1}$. The evolution of CO and $CO_2$ was monitored by a quadrupole mass spectrometer.

XAFS experiments were performed on the beam line 10B at the Photon Factory in the National Laboratory for High Energy Physics, Tsukuba, Japan. The synchrotron radiation from the storage ring (2.5 GeV, 350–250 mA) was monochromatized by a channel-cut Si(311) crystal monochromator and an energy resolution ($\Delta E/E$) was 0.0001. The samples were pressed into thin self-supporting wafers of 8-mm diameter and 2.2-mm thickness and mounted in a pyrex controlled-atmosphere spectroscopic cell with Kapton windows, where the sample was treated under different gas flows and temperatures. Unfocused transmitted X-ray beams were monitored using ionization chambers filled with appropriate gases. Spectra of Pt $L_{III}$ edge were recorded at RT after reduction or reaction with the samples still under the atmosphere of treating gases in the cell. In addition to catalyst samples, XAFS data were also obtained for Pt foil as a reference. XAFS data were analyzed by UWXAFS 2.0 package and FEFF6 code, licensed from University of Washington (13, 14).

The selective hydrodechlorination of CTC was carried out in a continuous isothermal flow reactor, fitted with a glass frit on which 200 mg of catalyst were placed. The reaction temperature of 393 or 413 K, and the molar ratio of reactants ($H_2$/CTC) was 5 or 9. The weight hourly space velocity (WHSV, liters CTC at STP/kg catalyst/h) was kept at 9000 liters/kg/h. Liquid CTC was vaporized in a saturator and carried by flowing hydrogen into the reactor. The temperature of the reactor was controlled by a proportional-integral-derivative (PID) temperature controller within $\pm 1$ K and the temperature of the saturator was controlled by a circulating bath within $\pm 0.1$ K. The effluent from the reactor was analyzed by an on-line gas chromatography (HP 5890 II) with a capillary column (AT-1, 30m $\times$ 0.3mm ID) and a flame ionization detector. To balance the amount of Cl, the formation of HCl during hydrodechlorination of CTC was titrated with standard 0.02 mole NaOH solution at vent stream. The conversion of CTC and selectivity toward formation of $CHCl_3$ was defined as follows:

$$\text{Conversion of CTC}(\%) = \frac{\text{moles CTC in} - \text{moles CTC out}}{\text{moles CTC in}} \times 100$$

$$\text{Selectivity to } CHCl_3(\%) = \frac{\text{moles } CHCl_3 \text{ out}}{\text{moles CTC in} - \text{moles CTC out}} \times 100.$$

## RESULTS

Table 1 shows the steady-state conversion of CTC and selectivity to $CHCl_3$, $CH_4$, and $C_2$ products over 1% Pt/$Al_2O_3$, at reaction temperature of 393 K and $H_2$/CTC mole ratio of 9 for 1% Pt/$Al_2O_3$, prepared from various Pt precursors. Except for the catalyst prepared from $K_2PtCl_6$, these three products accounted for more than 97% of the products and the balance was unidentified heavier products. The conversion of CTC exceeded 90% and selectivity to $CHCl_3$

**TABLE 1**

**Conversion and Selectivity over 1% Pt/$Al_2O_3$ Prepared from Various Pt Precursors at 393 K and $H_2$/CTC Mole Ratio of 9**

| Pt precursor | Conversion (%) | $CHCl_3$ (%) | $CH_4$ (%) | $C_2$ (%) | Specific rate[a] |
|---|---|---|---|---|---|
| $H_2PtCl_6$ | 97.6 | 69.0 | 22.6 | 5.7 | 0.264 |
| $K_2PtCl_6$ | 18.2 | 35.7 | 6.4 | 48.8 | 0.049 |
| $(NH_4)_2PtCl_6$ | 98.5 | 68.4 | 15.9 | 13.3 | 0.266 |
| $Pt(NH_3)_4Cl_2$ | 99.5 | 78.3 | 18.9 | 0.5 | 0.269 |
| $Pt(NH_3)_2(NO_2)_2$ | 99.5 | 78.4 | 20.6 | 0.4 | 0.269 |
| $Pt(NH_3)_4(NO_3)_2$ | 90.4 | 77.6 | 21.4 | 0.6 | 0.244 |

[a] Specific rate: CTC mol/Pt mol/h. Error range of conversion and selectivity: $\pm 1.0\%$.

**TABLE 2**

**Conversion and Selectivity over 1% $Pt/Al_2O_3$ Prepared from Various Pt Precursors at 413 K and $H_2$/CTC Mole Ratio of 9**

| Pt precursor | Conversion (%) | $CHCl_3$ (%) | $CH_4$ (%) | $C_2$ (%) | Specific rate[a] |
|---|---|---|---|---|---|
| $H_2PtCl_6$ | 99.8 | 59.8 | 29.6 | 9.5 | 0.269 |
| $K_2PtCl_6$ | 94.6 | 60.8 | 17.5 | 18.7 | 0.255 |
| $(NH_4)_2PtCl_6$ | 99.6 | 60.9 | 19.0 | 17.2 | 0.269 |
| $Pt(NH_3)_4Cl_2$ | 100.0 | 73.9 | 21.8 | 1.5 | 0.270 |
| $Pt(NH_3)_2(NO_2)_2$ | 100.0 | 72.8 | 24.6 | 1.0 | 0.270 |
| $Pt(NH_3)_4(NO_3)_2$ | 94.0 | 73.2 | 25.7 | 1.1 | 0.254 |

[a] Specific rate: CTC mol/Pt mol/h. Error range of conversion and selectivity: ±1.0%.

was higher than 65%, except for the catalyst derived from $K_2PtCl_6$. Especially, catalysts prepared from $Pt(NH_3)_4Cl_2$, $Pt(NH_3)_2(NO_2)_2$, and $Pt(NH_3)_4(NO_3)_2$ showed high $CHCl_3$ selectivity, better than 77%. Under these conditions, catalyst deactivation was not observed for 20 h of the reaction, except the $K_2PtCl_6$-derived catalyst. The catalyst prepared from $K_2PtCl_6$ deactivated with time on-stream and produced more than 50% of heavy compounds such as hexachloroethane ($C_2Cl_6$), tetrachloroethylene ($C_2Cl_4$), and unidentified heavier compounds. As a result, an exceptionally low $CHCl_3$ selectivity of 35.7% was recorded for this catalyst. Table 2 also shows the steady-state conversion of CTC and selectivity at reaction temperature of 413 K and $H_2$/CTC mole ratio of 9 for the same series of catalysts. At this higher temperature, the catalyst derived from $K_2PtCl_6$ also achieved high CTC conversion, more than 94%. Now the catalysts could be divided into two groups according to their selectivity. Catalysts prepared from $H_2PtCl_6$, $K_2PtCl_6$, and $(NH_4)_2PtCl_6$ (Group 1) showed selectivity to $CHCl_3$ of about 60% and those from $Pt(NH_3)_4Cl_2$, $Pt(NH_3)_2(NO_2)_2$, and $Pt(NH_3)_4(NO_3)_2$ (Group 2) showed higher selectivity to $CHCl_3$ of about 73%. The difference mainly came from the selectivity to $C_2$ compounds for which less selective catalysts prepared from $H_2PtCl_6$, $K_2PtCl_6$, and $(NH_4)_2PtCl_6$ showed much higher values than observed for selective catalysts. At 413 K, none of the catalysts showed deactivation for 20 h on stream.

In order to check the chlorine balance, the number of reacted Cl in a CTC molecule during hydrodechlorination was calculated from the conversion and selectivity as follows:

$$\text{No. of reacted Cl in a CTC molecule} = \text{Conversion (\%)} \times (S_{CH_4} \times 4 + S_{CH_2Cl_2} \times 2 + S_{CHCl_3})/10000.$$

Since Cl is removed as HCl in hydrodechlorination, the amount of HCl in the reaction effluent stream was titrated with a 0.02 mole NaOH solution. The amount of HCl by titration was nearly the same as the calculated amounts of Cl removed from CTC within ±5%.

To investigate the deactivation pattern, hydrogenation of CTC was carried out at severe reaction conditions of 413 K and $H_2$/CTC mole ratio of 5 and the conversion of CTC was plotted against time on-stream in Fig. 1. Under this condition of a low hydrogen concentration, all catalysts deactivated with time on-stream. Catalysts derived from $H_2PtCl_6$, $K_2PtCl_6$, and $(NH_4)_2PtCl_6$ deactivate rapidly as soon as the reaction starts; however, those from $Pt(NH_3)_4Cl_2$, $Pt(NH_3)_2(NO_2)_2$, and $Pt(NH_3)_4(NO_3)_2$ show much reduced rates of deactivation. Thus, the catalyst prepared from $K_2PtCl_6$ showed the most rapid deactivation and that from $Pt(NH_3)_2(NO_2)_2$ was the most stable among six catalysts from different Pt precursors. Hence, the results of deactivation pattern in Fig. 1 also divided the catalysts into two groups. Catalysts in Group 1 derived from $H_2PtCl_6$, $K_2PtCl_6$, and $(NH_4)_2PtCl_6$ are substantially more susceptible to deactivation, compared to catalysts in Group 2 derived from $Pt(NH_3)_4Cl_2$, $Pt(NH_3)_2(NO_2)_2$, and $Pt(NH_3)_4(NO_3)_2$. It is interesting to note that the grouping of the catalysts accroding to the selectivity is consistent with the grouping made according to deactivation. Thus, catalysts more selective to $CHCl_3$ appear to be more stable against deactivation.

Table 3 shows the percentage of Pt exposed to the surface and the particle size of platinum in 1% $Pt/Al_2O_3$ prepared from various Pt precursors measured by $H_2$ chemisorption and the particle size determined by TEM. The percentage of Pt exposed to the surface was high for all catalysts except for that prepared from $K_2PtCl_6$. The Pt particle sizes determined by TEM agreed well with Pt size calculated by $H_2$ chemisorption within ±10%. After 20 h of the hydrodechlorination reaction at 393 K with $H_2$/CTC of 9, the amount of chemisorbed hydrogen decreased from 0.98 H/Pt to 0.33 H/Pt for the catalyst derived from $H_2PtCl_6$

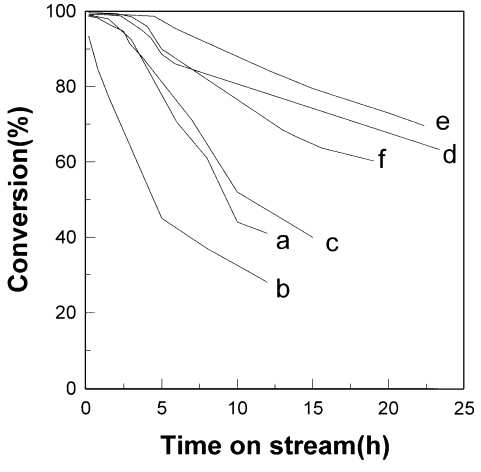


**FIG. 1.** Effects of Pt precursors on hydrodechlorination of CTC at 413 K, $H_2$/CTC mole ratio of 5, and WHSV of 9000 liters/kg/h: (a) $H_2PtCl_6$; (b) $K_2PtCl_6$; (c) $(NH_4)_2PtCl_6$; (d) $Pt(NH_3)_4Cl_2$; (e) $Pt(NH_3)_2(NO_2)_2$; (f) $Pt(NH_3)_4(NO_3)_2$.

**TABLE 3**

**Platinum Particle Size and Percentage of Pt Atom Exposed to the Surface in Fresh 1% $Pt/Al_2O_3$ Prepared from Various Pt Precursors**

| | $H_2$ chemisorption[a] | | TEM[b] |
|---|---|---|---|
| Pt precursor | Pt atom exposed (±3%) | Particle size(nm) (±0.05 nm) | Particle size(nm) (±0.2 nm) |
| $H_2PtCl_6$ | 97.9 | 0.92 | 1.0 |
| $K_2PtCl_6$ | 4.5 | 25.7 | 22.4 |
| $(NH_4)_2PtCl_6$ | 26.7 | 3.95 | 4.0 |
| $Pt(NH_3)_4Cl_2$ | 90.8 | 0.99 | 1.1 |
| $Pt(NH_3)_2(NO_2)_2$ | 45.2 | 1.98 | 2.0 |
| $Pt(NH_3)_4(NO_3)_2$ | 70.6 | 1.27 | 1.4 |

[a] The mean particle diameter ($d_p$) and percentage of Pt atom exposed ($D$) were calculated by the equations. $d_p = 5 \times V_M/a_M \times 100/D(\%)$; $D(\%) = 100 \times$ chemisorbed H/total Pt atoms, where $V_M$ is volume/Pt and $a_M$ is area/Pt.

[b] The mean particle diameter, $d_m$, was calculated by the equation $d_m = \Sigma n_i d_i / \Sigma n_i$, where $n_i$ is the number of particles of diameter $d_i$.

and from 0.45 H/Pt to 0.34 H/Pt for the catalyst made from $Pt(NH_3)_2(NO_2)_2$. TEM also indicated that the size and shape of Pt particles remained almost the same in all catalysts after reaction at the same reaction conditions.

The BET surface areas $S_g$ of 1% $Pt/Al_2O_3$ are shown in Table 4. The $S_g$ of all the fresh catalyst were almost the same ($95 \pm 2$ $m^2/g$), and they were also identical to the support $\gamma$-$Al_2O_3$ itself, regardless of the Pt precursors. The surface areas of the catalysts decreased after the reaction. However, the relationship between deactivation behavior of the catalysts and the surface areas of the used catalysts was not apparent.

Figure 2 shows the results of TPR of 1% $Pt/Al_2O_3$. Prior to TPR, samples impregnated with different precursor solutions were dried at 383 K for 24 h, calcined in $O_2$ flow at 573 K for 2–3 h, and then treated in He flow at 773 K for 2 h to remove impurities such as water or organics. There were two $H_2$ consumption peaks, one at low temperature between 473 and 573 K and the other at high temperature

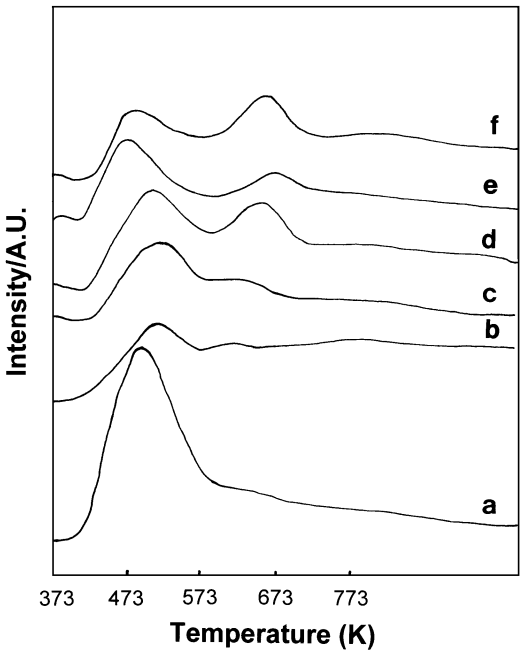


**FIG. 2.** TPR spectra of 1% $Pt/Al_2O_3$ prepared from various Pt precursors at heating rate of 10 K/min: (a) $H_2PtCl_6$; (b) $K_2PtCl_6$; (c) $(NH_4)_2PtCl_6$; (d) $Pt(NH_3)_4Cl_2$; (e) $Pt(NH_3)_2(NO_2)_2$; (f) $Pt(NH_3)_4(NO_3)_2$.

near 673 K. From the results of TPR, Pt precursors over 1% $Pt/Al_2O_3$ could be also divided into two groups. The catalysts prepared from Group 1 Pt precursors did not show any significant intensity for the reduction peak at 673 K. However, the catalysts prepared from Group 2 Pt precursors showed strong reduction peak at 673 K whose intensity was comparable to that of the low temperature reduction peak.

Table 5 shows the results of chemical analysis (CA) and atomic concentration of C and Cl in fresh, used, and

**TABLE 4**

**BET Surface Area ($m^2\ g^{-1}$) of 1% $Pt/Al_2O_3$ Prepared from Various Pt Precursors**

| Pt precursor | Fresh (±2 $m^2/g$) | Used[a] (±2 $m^2/g$) |
|---|---|---|
| $H_2PtCl_6$ | 95 | 87 |
| $K_2PtCl_6$ | 95 | 62 |
| $(NH_4)_2PtCl_6$ | 95 | 72 |
| $Pt(NH_3)_4Cl_2$ | 95 | 75 |
| $Pt(NH_3)_2(NO_2)_2$ | 95 | 84 |
| $Pt(NH_3)_4(NO_3)_2$ | 95 | 70 |

[a] At 393 K, $H_2/CCl_4$ mole ratio of 9, and WHSV of 9000 liters/kg/h for 20 h.

**TABLE 5**

**Chemical Analysis (wt%) and Atomic Concentration (%) of C and Cl by XPS for $Pt/Al_2O_3$ Catalyst Prepared from $H_2PtCl_6$**

| | Fresh | Used[a] | Deactivated[b] |
|---|---|---|---|
| Chemical analysis (±0.01 wt%) | | | |
| C | 0.06 | 0.37 | 2.03 |
| Cl | 0.065 | 0.068 | 0.070 |
| Atomic concentration (±0.5%) | | | |
| Al[c] | 37.90 | 36.88 | 32.05 |
| C[d] | 6.70 | 10.79 | 20.68 |
| Cl[e] | 1.27 | 1.70 | 1.85 |

[a] Used for steady-state hydrodechlorination at 393 K and $H_2$/CTC mole raio of 9 for 5 h.

[b] Used for hydrodechlorination at 413 K and $H_2$/CTC mole ratio of 5 for 10 h, where the catalyst showed a continuous deactivation.

[c] From $Al_{2p}$ peak with a sensitivity factor of 0.234.

[d] From $C_{1s}$ peak with a sensitivity factor of 0.296.

[e] From $Cl_{2p}$ peak with a sensitivity factor of 0.891.

deactivated 1% $Pt/Al_2O_3$, determined by XPS analysis. The used catalysts had shown a steady-state activity without any sign of deactivation at 393 K, $H_2$/CTC mole ratio of 9 for 5 h. The $Pt/Al_2O_3$ catalyst was prepared from $H_2PtCl_6$. The deactivated catalyst, on the other hand, had shown a strong tendency of deactivation at 413 K and $H_2$/CTC mole ratio of 5 for 5 h. As XPS is a surface sensitive technique, the atomic concentration of C and Cl is different from the results of CA. The atomic concentration of Al was used as a reference to compare the relative amounts of C and Cl. Hence, the relative values for different samples should be considered. The amounts of carbon by CA increased ramarkably in deactivated catalyst compared to fresh and steady-state catalyst. However, the chlorine contents in fresh, steady-state, and deactivated catalyst by CA was nearly same. On the other hand, the atomic concentrations of C and Cl measured by XPS increased at steady state and in the deactivated catalyst compared to those in the fresh catalyst. In particular, the increase of C concentration was much higher than the increase of Cl concentration. This trend observed in XPS analysis is consistent with that in CA results.

Figures 3 and 4 show $CO_2$ evolution by TPO of 1% $Pt/Al_2O_3$ prepared from $H_2PtCl_6$ and $Pt(NH_3)_2(NO_2)_2$ as Pt precursors. The $CO_2$ evolution was observed between 470 K and 700 K. For steady-state samples, $Pt/Al_2O_3$ derived from $H_2PtCl_6$ showed a greater amounts of $CO_2$ evolution than the catalyst prepared from $Pt(NH_3)_2(NO_2)_2$. However, the amounts of $CO_2$ evolved from the deactivated catalysts were nearly the same for catalysts prepared from $H_2PtCl_6$ or $Pt(NH_3)_2(NO_2)_2$.

In order to obtain further information on the state and structure of Pt in $Pt/Al_2O_3$ catalyst prepared from different Pt precursors, the technique of XAFS was employed. Figure 5 compares Pt $L_{III}$ X-ray absorption near edge structure (XANES) of fresh catalysts prepared from various precursors with that of Pt foil as a reference sample. The general shape of XANES spectra of catalysts was similar to that of Pt foil, except those prepared from $Pt(NH_3)_2(NO_2)_2$ and $Pt(NH_3)_4Cl_2$, which did not show two peaks at 11575 and 11590 eV due to multiple scattering resonance. However, the edge position (the first inflection point on the rapidly rising portion of the absorption edge) and white line area (the intensity of the absorption peak) were markedly different among $Pt/Al_2O_3$ derived from different Pt precursors. The quantitative results are summarized in Table 6. In general, the edge position shifts to a higher energy and white line area increases as the oxidation number of the absorber

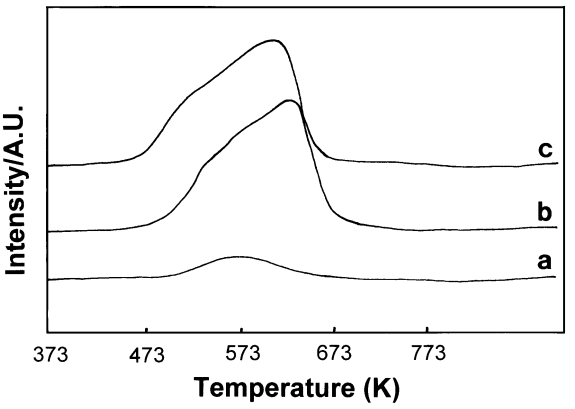


**FIG. 4.** $CO_2$ evolution by TPO of 1% $Pt/Al_2O_3$ used for hydrodechlorination at 413 K with $H_2$/CTC of 5 for 20 h, which showed catalyst deactivation: (a) $Al_2O_3$; (b) $Pt/Al_2O_3$ derived from $Pt(NH_3)_2(NO_2)_2$; (c) $Pt/Al_2O_3$ derived from $H_2PtCl_6$.

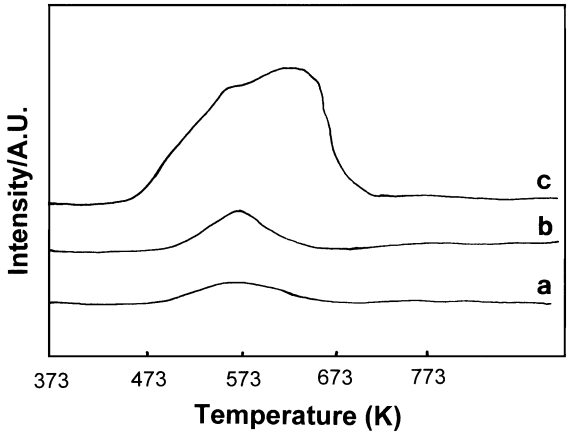


**FIG. 3.** $CO_2$ evolution by TPO of 1% $Pt/Al_2O_3$ used for steady-state hydrodechlorination at 393 K with $H_2$/CTC of 9 for 20 h. The flow rate of 20 ml $min^{-1}$: 15 $\mu$mol $s^{-1}$, heating rate: 10 K $min^{-1}$. (a) $Al_2O_3$ alone; (b) $Pt/Al_2O_3$ derived from $Pt(NH_3)_2(NO_2)_2$; (c) $Pt/Al_2O_3$ derived from $H_2PtCl_6$.

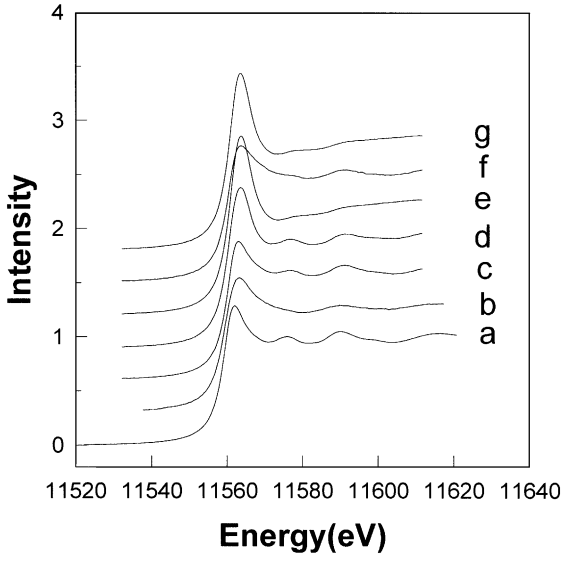


**FIG. 5.** XANES spectra of Pt $L_{III}$ edge for fresh 1% $Pt/Al_2O_3$ prepared from various precursors: (a) Pt foil; (b) $H_2PtCl_6$; (c) $(NH_4)_2PtCl_6$; (d) $K_2PtCl_6$; (e) $Pt(NH_3)_2(NO_2)_2$; (f) $Pt(NH_3)_4(NO_3)_2$; (g) $Pt(NH_3)_4Cl_2$.

**TABLE 6**

**The Edge Energies and White Line Areas of Fresh Catalysts and Catalysts Used for the Steady-State Reaction at 393 K, $H_2$/CTC Mole Ratio of 9 for 5 h**

| | Edge energy[a] | | White line area[b] | |
|---|---|---|---|---|
| Pt precursor | Fresh | Used | Fresh | Used |
| $H_2PtCl_6$ | 11560.8 | 11560.4 | 1.11 | 1.08 |
| $K_2PtCl_6$ | 11560.7 | 11560.5 | 1.07 | 1.02 |
| $(NH_4)_2PtCl_6$ | 11560.4 | 11560.4 | 1.03 | 0.98 |
| $Pt(NH_3)_4Cl_2$ | 11561.0 | 11560.5 | 1.10 | 1.05 |
| $Pt(NH_3)_2(NO_2)_2$ | 11561.1 | 11560.5 | 1.11 | 1.05 |
| $Pt(NH_3)_4(NO_3)_2$ | 11560.6 | 11560.6 | 1.06 | 1.05 |

[a] Edge energy: ±0.1 eV.
[b] Relative white line area ($A_{sample}/A_{Pt\ foil}$): ±0.01.

metal is raised (15–19). The edge position and white line areas of all fresh catalysts were higher than those for Pt foil.

Figure 6 shows Pt $L_{III}$ XANES of $Pt/Al_2O_3$ after steady-state hydrodechlorination of CTC at 393 K with $H_2$/CTC of 9 for 5 h. Again, the general shape of XANES spectra was all similar to that of Pt foil. The quantitative results are also summarized in Table 6. The edge positions of all catalysts were higher than Pt foil and nearly same regardless of Pt precursors. However, the white line areas of catalysts after steady-state reaction were different according to Pt precursors and could be classified into two groups. Group 2 catalysts which showed excellent $CHCl_3$ selectivity and stability in hydrodechlorination had white line areas close to 1.05. Less effective Group 1 catalysts had either smaller ($K_2PtCl_6$, $(NH_4)_2PtCl_6$) or larger ($H_2PtCl_6$) white line areas.

Small oscillations above the absorption edge are called extended X-ray absorption fine structure (EXAFS). The

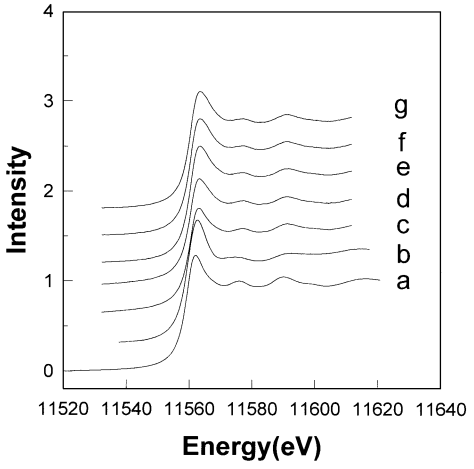


**FIG. 6.** XANES spectra of Pt $L_{III}$ edge for 1% $Pt/Al_2O_3$ prepared from various precursors and used for the steady-state hydrodechlorination at 393 K and $H_2$/CTC mole ratio of 9 for 5 h: (a) Pt foil; (b) $H_2PtCl_6$; (c) $(NH_4)_2PtCl_6$; (d) $K_2PtCl_6$; (e) $Pt(NH_3)_2(NO_2)_2$; (f) $Pt(NH_3)_4(NO_3)_2$; (g) $Pt(NH_3)_4Cl_2$.

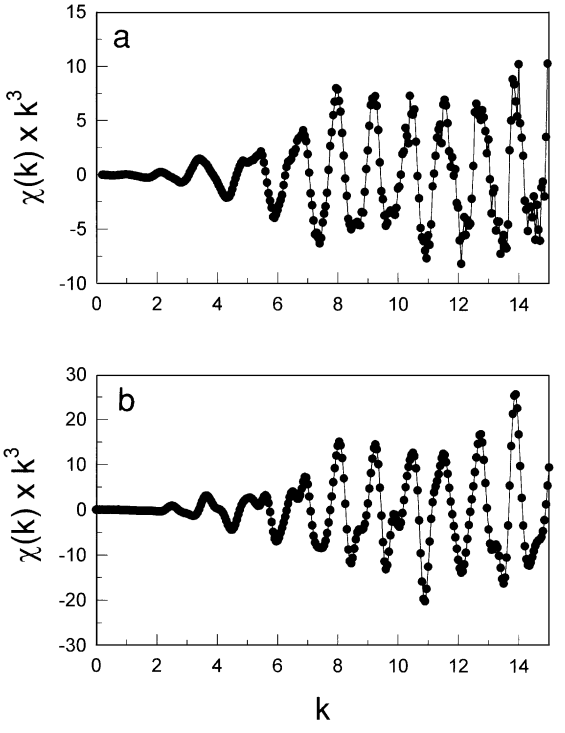


**FIG. 7.** Background subtracted $k^3$ weighted EXAFS of used 1% $Pt/Al_2O_3$ derived from $Pt(NH_3)_2(NO_2)_2$ (a) and Pt foil (b).

EXAFS signals, $\chi(k)$, was isolated from the background absorption. This EXAFS was weighted by $k^3$ ($k/A^{-1}$ = wave vector). To enhance the accuracy of the EXAFS data, any discontinuities such as glitches were removed before background removal. Figure 7 compares the normalized EXAFS data for Pt foil and the 1% $Pt/Al_2O_3$ catalyst derived from $Pt(NH_3)_2(NO_2)_2$ and used for the steady-state hydrodechlorination. To obtain radial structure functions (RSFs), $k^3\chi(k)$ was Fourier-transformed. The range of k for Fourier-transformation was from 2 to 15 $Å^{-1}$. Figure 8 shows RSF of catalysts in the fresh state (solid lines) and after the steady-state reaction (dotted lines). The peak around 0.27 nm that could be assigned to Pt–Pt interaction are well developed for fresh catalysts prepared from $H_2PtCl_6$, $K_2PtCl_6$, $(NH_4)_2PtCl_6$, and $Pt(NH_3)_4(NO_3)_2$. But, the Pt–Pt peak was very small for $Pt(NH_3)_2(NO_2)_2$ and $Pt(NH_3)_4Cl_2$. The latter two samples, thus, possess a poorly developed bulk structure as also suggested by the absence of multiple scattering resonance in XANES shown in Fig. 5. After the steady-state reaction, the Pt–Pt peak was more clearly developed than for fresh Group 2 catalysts. In particular, the Pt–Pt intensity for the catalysts prepared from $Pt(NH_3)_4Cl_2$ and $Pt(NH_3)_2(NO_2)_2$ was now sharply increased. On the other hand, the intensity for the catalyst derived from $H_2PtCl_6$ was reduced dramatically. Table 7 summarizes the results of EXAFS curve fitting for Pt–Pt interaction by the *r*-space method (13, 14) with range of *r*

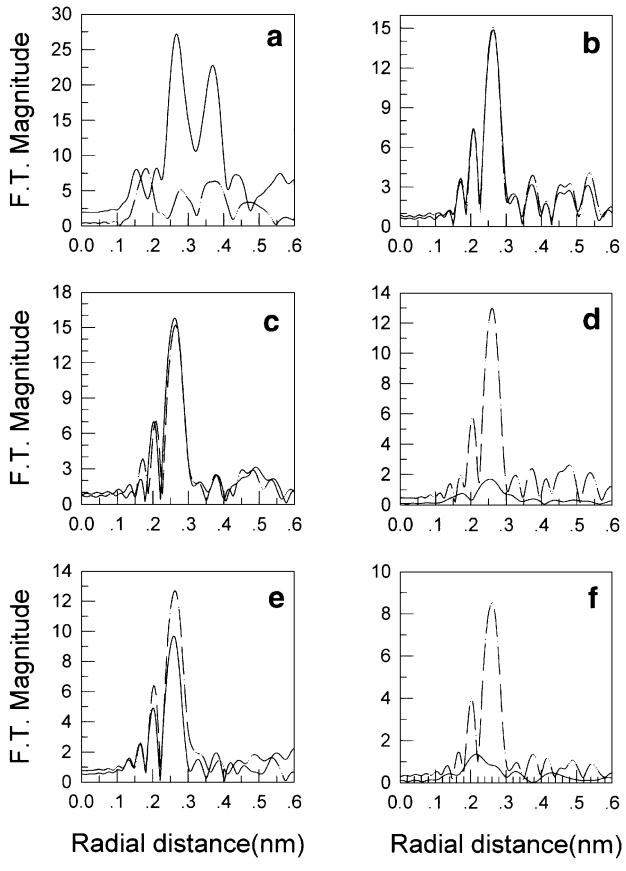


**FIG. 8.** RSF of 1% $Pt/Al_2O_3$ prepared from various precursors. Solid line: fresh catalyst; dotted line: used catalyst (393 K, $9(H_2/CCl_4)$). (a) $H_2PtCl_6$; (b) $K_2PtCl_6$; (c) $(NH_4)_2PtCl_6$; (d) $Pt(NH_3)_2(NO_2)_2$; (e) $Pt(NH_3)_4(NO_3)_2$; (f) $Pt(NH_3)_4Cl_2$.

from 2 to 3.5 Å. The values of coordination numbers and Debye–Waller factors are also given in Table 7. The Pt–Pt coordination number of Group 1 catalysts decreased and that of Group 2 catalysts increased after the reaction. Especially, the Pt–Pt coordination number of catalysts derived from $Pt(NH_3)_4Cl_2$ and $Pt(NH_3)_2(NO_2)_2$ increased dramatically and that of $H_2PtCl_6$ decreased sharply, all in agreement with the RSF results shown in Fig. 8.

## DISCUSSION

In the hydrodechlorination of CTC, the main factors to be considered are the selectivity to $CHCl_3$ and the stability of the catalyst during the reaction. In our previous studies (9, 10), where $H_2PtCl_6$ was employed as a Pt precursor, MgO was found to be the best support, giving the highest selectivity toward formation of $CHCl_3$ and good maintenance of the catalytic activity among various supports, including MgO, $Al_2O_3$, $SiO_2$, $TiO_2$, $ZrO_2$, silica-alumina, and Na ion-exchanged Y-type zeolite. The present work demonstrated that $\gamma$-$Al_2O_3$ could also be the support of choice for the selective hydrodechlorination of CTC to $CHCl_3$ if a proper Pt precursor such as $Pt(NH_3)_4Cl_2$, $Pt(NH_3)_2(NO_2)_2$, or $Pt(NH_3)_4(NO_3)_2$ was employed.

For comparison, the 1% Pt/MgO catalyst employed in our previous studies (9, 10) showed CTC conversions of 27% and 90%, and $CHCl_3$ selectivity of 64% and 71% at 393 K and 413 K, respectively, under otherwise identical reaction conditions employed in the present work. It is obvious from Tables 1 and 2 that several 1% $Pt/Al_2O_3$ catalysts are more active and more selective than the 1% Pt/MgO. Furthermore, alumina-supported catalysts have no complications which might be caused by the phase change of the support. In MgO-supported catalysts, MgO transforms into $MgCl_2 \cdot xH_2O$ during hydrodechlorination (10). Most importantly, the excellent activity and selectivity of $Pt/Al_2O_3$ catalysts are maintained like Pt/MgO during 20 h of our experiments.

It is rather surprising that precursors employed in the preparation of $Pt/Al_2O_3$ catalysts exert such a profound influence on the performance of the resulting catalysts. According to the results of hydrodechlorination of CTC shown in Tables 1 and 2 and Fig. 1, six precursors employed in the present study could be classified into two groups. The Group 1 precursors of $H_2PtCl_6$, $K_2PtCl_6$, and $(NH_4)_2PtCl_6$ yield $Pt/Al_2O_3$ catalysts which are less selective to $CHCl_3$ and less stable against the activity loss during the reaction than the catalysts derived from Group 2 precursors of $Pt(NH_3)_4Cl_2$, $Pt(NH_3)_2(NO_2)_2$, and $Pt(NH_3)_4(NO_3)_2$. More interestingly, $Pt/Al_2O_3$ catalysts prepared from the precursors of different groups behave distinctively, while those from the same group behave similarly in catalyst characterization experiments of TPR and XAFS. Of course, the Group 1 precursors have the formal oxidation state of Pt(IV) while the Group 2 precursors contain Pt(II), although these initial oxidation states of Pt are not likely to be retained in the $Pt/Al_2O_3$

**TABLE 7**

**Results of EXAFS Curve Fitting for Pt–Pt Interaction for the Fresh Catalysts and Catalysts Used for the Steady-State Reaction at 393 K, $H_2$/CTC Mole Ratio of 9 for 5 h**

| | Pt–Pt distance[a] (nm) | | Pt coordination[b] number | | Debye–Waller factor[c] | |
|---|---|---|---|---|---|---|
| Pt precursor | Fresh | Used | Fresh | Used | Fresh | Used |
| $H_2PtCl_6$ | 0.273 | 0.284 | 8.5 | 1.7 | 0.001037 | 0.002612 |
| $K_2PtCl_6$ | 0.276 | 0.276 | 5.7 | 5.5 | 0.004139 | 0.006245 |
| $(NH_4)_2PtCl_6$ | 0.276 | 0.276 | 8.8 | 6.6 | 0.005193 | 0.004540 |
| $Pt(NH_3)_4Cl_2$ | 0.276 | 0.276 | 3.0 | 9.0 | 0.002557 | 0.003814 |
| $Pt(NH_3)_2(NO_2)_2$ | 0.280 | 0.275 | 2.3 | 9.2 | 0.008634 | 0.006735 |
| $Pt(NH_3)_4(NO_3)_2$ | 0.275 | 0.276 | 5.9 | 6.2 | 0.006195 | 0.004374 |
| Pt foil | 0.278 | | 12.0 | | 0.004987 | |

[a] Pt–Pt distance: ±0.0005 nm.

[b] Pt–Pt coordination number: ±0.2.

[c] Relative to Pt foil, i.e., $\Delta\sigma^2$(sample) − $\Delta\sigma^2$(Pt foil): ±0.00001.

catalyst after the calcination and reduction processes that structure all catalysts have undergone before the reaction.

Before discussing the oxidation state and the structure of each catalyst probed by TPR and XAFS, let us discuss here the cause of catalyst deactivation in hydrodechlorination of CTC. Deactivated catalysts showed severely suppressed hydrogen chemisorption. Thus, hydrogen chemisorption for $Pt/Al_2O_3$ prepared from $H_2PtCl_6$ decreased from 0.98 H/Pt for the fresh catalyst to 0.33 H/Pt for the catalyst used in the steady-state reaction at 393 K and $H_2$/CTC mole ratio of 9, and then to 0.05 H/Pt for the catalyst deactivated by the reaction at 413 K and $H_2$/CTC mole ratio of 5 for 20 h. Similarly, the hydrogen chemisorption on the catalyst prepared from $Pt(NH_3)_2(NO_2)_2$ also decreased from the initial value of 0.45 H/Pt to 0.34 H/Pt when used in the steady-state reaction and to 0.05 H/Pt when deactivated. The reduced amount of hydrogen chemisorption is not due to the growth of Pt particles in the used and deactivated catalysts. The particle size of Pt remained essentially the same as seen by TEM in fresh, used, and deactivated catalysts.

Another potential cause of the deactivation is chlorine (20–23) which originates from the Pt precursor or the reactant CTC. The amount of chlorine was measured by chemical analysis and XPS and is shown in Table 5. Since XPS is a surface sensitive technique with a probing of ca 2–4 nm and chemical analysis is a bulk technique, the absolute values of chlorine measured by the two techniques are different. Yet, the trend is consistent. The chlorine content in the deactivated catalyst was almost the same as that in the used catalyst for which no sign of deactivation was detected. Hence, the presence of chlorine is not the cause of the catalyst deactivation. It is believed that the Pt catalyst is deactivated due to coking in the hydrodechlorination of CTC as proposed by Wang *et al.* (24–27) and also found by us for Pt/MgO catalysts (9, 10). Both chemical analysis and XPS analysis in Table 5 demonstrated that the content of carbon is the major difference between the used and deactivated catalysts. The results of TPO shown in Fig. 3 also indicate that the $Pt/Al_2O_3$ catalyst prepared from $Pt(NH_3)_2(NO_2)_2$ shows suppressed coke formation on the Pt during the hydrodechlorination, compared to the catalyst prepared from $H_2PtCl_6$. This difference in amount of $CO_2$ evolution appears to be correlated with the catalyst deactivation pattern among Pt precursors shown in Fig. 1. Of course, all deactivated catalysts showed the similar large amounts of coke formation irrespective of their precursors, as shown in Fig. 4. Finally, it has also been reported that deactivated Pt catalysts could be regenerated by oxygen treatment at 573 K for 3 h (28–30).

Examination of Tables 1 and 2 and Fig. 1 indicates that the rapid deactivation of $Pt/Al_2O_3$ in the hydrodechlorination of CTC at severe reaction conditions (413 K, $H_2$/CTC mole ratio of 5) goes hand in hand with enhanced production of $C_2$ products. The formation of $C_2$ or heavier compounds in the dydrodechlorination of CTC was confirmed with a gas chromatography–mass spectrometer analysis. Substantial amounts of $C_2$ products are formed over 1% $Pt/Al_2O_3$ prepared from $H_2PtCl_6$, $K_2PtCl_6$, and $(NH_4)_2PtCl_6$, where rapid catalyst deactivation is observed. The boiling point of $C_2Cl_4$ is 394 K and that of $C_2Cl_6$ is 459.8 K. Thus, it is highly plausible to assume that high boiling oligomers ($C_2$ and heavier) are the precursors to coke formed over the $Pt/Al_2O_3$ catalyst. Keeping this apparent correlation between selectivity and deactivation behavior of $Pt/Al_2O_3$ in mind, let us now discuss the structure and oxidation state of Pt.

The first distinction that each Pt precursor belonging to Groups 1 and 2 makes is its formal oxidation state. The Group 1 precursors are in Pt(IV) state and the Group 2 precursors in Pt(II) state. As mentioned, this nice grouping, however, may be a coincidence because the preparation of $Pt/Al_2O_3$ from these precursors involves a number of chemical treatments that might erase this initial difference in the formal oxidation state. TPR of 1% $Pt/Al_2O_3$ prepared from Pt(IV) precursors (Group 1) showed a large reduction peak at a low temperature between 473–573 K. However, TPR of 1% $Pt/Al_2O_3$ prepared from Pt(II) precursors (Group 2) showed two large reduction peaks, one at a low temperature between 473–573 K and the other at a high temperature of about 673 K. This is in a good agreement with the observation reported in the literature concerning the reduction of oxidized Pt species supported in $Al_2O_3$ (31–41). The reduction peak at low temperatures has been interpreted as due to a three-dimensional platinum oxide phase, which does not interact with $Al_2O_3$, and that at high temperatures, due to a two-dimensional complex platinum oxide phase (either $Pt–Al_2O_3–Cl$ or $PtO_2–Al_2O_3$), which interacts strongly with $Al_2O_3$. A consequence of the different reducibility among different precursors is that the Pt catalyst prepared from Pt(IV) precursors should have been reduced to a greater extent by reduction at 573 K than those from Pt(II) precursors. In any case, the state of $Pt/Al_2O_3$ examined by TPR represents the state of calcined catalysts, or at best, that of a fresh catalyst if the reduction is also considered. On the other hand, the state of a catalyst under the steady-state reaction conditions should be the most relevent to its catalytic behavior in the hydrodechlorination of CTC.

As shown by XAFS, a substantial change in the oxidation state and structure takes place during the hydrodechlorination reaction. Both the edge position and white line area of Pt $L_{III}$ XANES over 1% $Pt/Al_2O_3$ prepared from different Pt precursors shown in Figs. 5 and 6 and Table 6 indicate that Pt in the fresh catalysts has a higher oxidation state than Pt in the used catalysts. This means that the catalysts are partially reduced during hydrodechlorination. Although the edge position of all catalysts at steady state was nearly the same, the white line area was different, depending on the Pt precursors. The catalysts prepared from Pt(II) precursors

have nearly the same white line area, close to 1.05 relative to the Pt foil. The same white line area was measured for authentic $PtCl_2$ (10, 42). On the other hand, the white line areas of $Pt/Al_2O_3$ catalysts prepared from Pt(IV) precursors were either larger (ca 1.08 for $H_2PtCl_6$) or smaller (close to 1.0 for $K_2PtCl_6$ and $(NH_4)_2PtCl_6$). Considering the fact that the white line area of Pt $L_{III}$ XANES represents the oxidation state of Pt, one may conclude that the optimal oxidation state of Pt that gives rise to the best $CHCl_3$ selectivity and stability is the one presented by the white line area of 1.05. Deviation from this optimum is not desirable. A higher value appears to bring about the enhanced $CH_4$ selectivity as exemplified by the catalyst prepared from $H_2PtCl_6$. A lower value seems to promote the formation of $C_2$ products as evidenced for $K_2PtCl_6$ and $(NH_4)_2PtCl_6$. The white line areas for the last two samples are close to that of Pt foil (1.00), indicating almost complete reduction of the Pt in the catalysts.

In Fig. 8, RSF of the fresh catalysts indicates that the catalysts prepared from Pt(II) precursors were less reduced than those from Pt(IV) precursors in agreement with the expectation based on the TPR results in Fig. 2. During hydrodechlorination the catalysts prepared from Pt(II) precursors were further reduced as indicated by the increased Fourier transformation (F.T.) magnitude of the Pt–Pt interaction. Except for the catalyst prepared from $H_2PtCl_6$ which showed poorly defined RSF, all the catalysts showed the bulk structure of metallic Pt similar to Pt foil. There is no apparent correlation between structural characteristics determined by EXAFS and catalytic behavior of the catalysts in the hydrodechlorination of CTC.

XAFS results showed that probably the most important factor determining catalytic performance of 1% $Pt/Al_2O_3$ is the oxidation state of Pt during the steady-state hydrodechlorination of CTC. Different precursors lead to different oxidation states in working catalysts (31, 32, 34, 41). Since L-edge X-ray absorption of Pt takes place due to electron transition from *p* states to *d* states of Pt, white line area is proportional to the number of *d*-vacancies of Pt in the sample (15–19). Thus, a higher value for the white line area represents a higher oxidation state. Then, it appears that Pt in a high oxidation state promotes the formation of $CH_4$ and Pt in a low oxidation state leads to the preferred formation of $C_2$'s. Pt in an intermediate oxidation state is needed to obtain the best selectivity to $CHCl_3$. Let us rationalize this observed correlation between selectivity and thus stability of $Pt/Al_2O_3$ in hydrodechlorination of CTC with the oxidation state of Pt.

The mechanism of hydrodechlorination of CTC is not well understood. Weiss *et al.* (1, 43) studied the hydrogenation of CTC over $Pt/\eta$-$Al_2O_3$ and Ni ion-exchanged Y-type zeolite (NiY). The experimental results over $Pt/\eta$-$Al_2O_3$ showed selective hydrogenation of CTC to $CHCl_3$ and $CH_4$. The reactivity of intermediate products, $CHCl_3$, $CH_2Cl_2$, and $CH_3Cl$, was below 10% of the reactivity of CTC. The authors proposed that the reaction of CTC with $H_2$ over the $Pt/\eta$-$Al_2O_3$ catalyst proceeded via two parallel routes, producing $CHCl_3$ and $CH_4$ at a constant mole ratio independent of process variables. Namely, the formation of $*CCl_3$ surface radical ($*$ denotes Pt site) is the initial step and hydrogen addition to adsorbed $*CCl_3$ accounts for $CHCl_3$. The concerted Cl abstraction and hydrogen addition to $*CCl_3$ with no important desorption of intermediates account for $CH_4$. Over NiY, $C_2$ ($C_2Cl_2H_4$, $C_2Cl_4H_2$, and $C_2Cl_6$) and $C_3$ ($C_3Cl_2H_6$) products were produced by oligomerization of free-radicals. The essential feature of the mechanism could be presented by the following scheme:

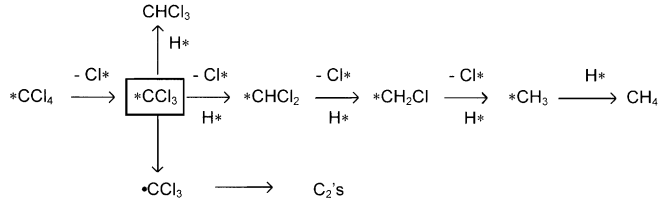


**SCHEME 1**

The selectivity among $CHCl_3$, $CH_4$, and $C_2$'s is determined by the fate of the adsorbed intermediate $*CCl_3$. Two factors are potentially important in this process; the binding energy of $*CCl_3$ with the Pt surface and the availability of adsorbed hydrogen H$*$. For example, deficiency of H$*$ could lead to oligomerization of $*CCl_3$ to $C_2$'s. The dissociative chemisorption most rapidly occurs on metallic Pt, hence, on $Pt/Al_2O_3$ catalysts derived from $K_2PtCl_6$ and $(NH_4)_2PtCl_6$. The preferred formation of $C_2$'s over these catalysts suggests that the availability of H$*$ is not an important factor in determining selectivity of $Pt/Al_2O_3$. The binding energy of $*CCl_3$ is expected to increase as the number of *d*-vacancies is increased and, thus, be the largest for $Pt/Al_2O_3$ derived from $H_2PtCl_6$. A large binding energy results in a long residence time of $*CCl_3$ on the surface and will lead to a higher chance of $CH_4$ formation by extensive dechlorination and hydrogenation. This is, indeed, what is observed for $Pt/Al_2O_3$ derived from $H_2PtCl_6$. A small binding energy would promote the desorption of $*CCl_3$ to form a free radical $\cdot CCl_3$ which could oligomerize into $C_2$'s. Again, this is consistent with the preferred formation of $C_2$'s over $Pt/Al_2O_3$ prepared from $K_2PtCl_6$ and $(NH_4)_2PtCl_6$ which showed the low oxidation state close to Pt(0). The three catalysts derived from Group 2 precursors possess the intermediate oxidation state and are expected to have an optimal binding energy that would yield the best $CHCl_3$ selectivity (44–46).

The oxidation state of Pt in $Pt/Al_2O_3$ might have been better probed by more surface sensitive XPS rather than XANES. Unfortunately, Pt $4f_{7/2}$ peak at 71.2 eV is

completely masked by dominating Al 2*p* peak from $\gamma$-$Al_2O_3$ (47).

## CONCLUSION

The 1% $Pt/Al_2O_3$ catalyst is effective in the hydrodechlorination of CTC to $CHCl_3$ with high activity, selectivity, and stability when a proper Pt precursor is chosen. The Pt(II) precursors such as $Pt(NH_3)_4Cl_2$, $Pt(NH_3)_2(NO_2)_2$, and $Pt(NH_3)_4(NO_3)_2$ yield catalysts which show stable operation with CTC conversions close to 100% and $CHCl_3$ selectivity above 78% at 393 K, $H_2$/CTC mole ratio of 9, and WHSV of 9000 liters/kg/h. The reason for the difference between different precursors appears to be the oxidation state of Pt in the prepared $Pt/Al_2O_3$ catalyst during the steady-state reaction.

## REFERENCES


1. Weiss, A. H., Gambhir, B. S., and Leon, R. B., *J. Catal.* **22**, 245 (1971).
2. Helland, B. R., Alvarez, P. J. J., and Schnoor, J. L., *J. Hazard. Mat.* **41**, 205 (1995).
3. Holbrook, M. T., and Harley, D. A., E.P. 0,479,116,A1 (1991).
4. Dogimont, C., Franklin, J., Janssens, F., Schoebrechts, J. P., and Doiceau, G., U.S.P. 5,146,013 (1992).
5. Miguel, E. T., Gimenez, M. S., Arroyo, A. C., Gomex, L. S., and Martin, A., W.O. 91/09827 (1991) and U.S.P. 5,208,393 (1993).
6. Petrosky, J. T., Vulcan Material Com., U.S.P. 5,315,050 (1994).
7. Morikawa, S., Yoshitake, M., and Tatematsu, S., J.P. 4-305538, J.P. 4-305539, and J.P. 4-305540 (1992).
8. Suzuki, T., and Kawaru, S., J.P. 4-364136 (1992).
9. Kim, S. Y., Choi, H. C., Yang, O. B., Lee, K. H., Lee, J. S., and Kim, Y. G., *J. Chem. Soc., Chem. Commun.*, 2169 (1995).
10. Choi, H. C., Choi, S. H., Yang, O. B., Lee, J. S., Lee, K. H., and Kim, Y. G., *J. Catal.* **161**, 790 (1996).
11. Kim, Y. G., "An Introduction to Chemical Reaction Engineering," Han rym won, Seoul, 1990.
12. Rouabah, D., and Fraissard, J., *J. Catal.* **144**, 30 (1993).
13. Rehr, J. J., de Leon, J. M., Zabinsky, S. I., and Albers, R. C., *J. Am. Chem. Soc.* **113**, 5135 (1991).
14. O'Day, P. A., Rehr, J. J., Zabinsky, S. I., and Brown, G. E., Jr., *J. Am. Chem. Soc.* **116**, 2938 (1994).
15. Koningsberger, D. C., and Prins, R. (Eds.), "X-ray Absorption: Principles, Applications and Techniques of EXAFS, SEXAFS, and XANES," Wiley, New York, 1988.
16. Lytle, F. W., Wei, P. S. P., Greegor, R. B., Via, G. H., and Sinfelt, J. H., *J. Chem. Phys.* **70**, 4849 (1979).
17. Horsley, J. A., *J. Chem. Phys.* **76**, 1451 (1982).
18. Mattheiss, L. F., and Dietz, R. E., *Phys. Rev. B* **22**, 1663 (1980).
19. Teo, B. K., "EXAFS: Basic Principles and Data Analysis," Springer-Verleg, New York/Berlin, 1986.
20. Windawi, H., and Wyatt, M., *Platinum Metals Rev.* **37**(4), 186 (1993).
21. Spirey, J. J., and Butt, J. B., *Catal. Today* **11**, 465 (1992).
22. Bozena, M. K., Anna, M. P., and Krystina, S., *Catal. Today* **11**, 597 (1992).
23. Bozzelli, J. W., and Chen, Y. M., *Chem. Eng. Comm.* **115**, 1 (1992).
24. Wang, Y. N., Macros, J. A., Simmons, and Klier, K., *J. Phys. Chem.* **94**, 7597 (1990).
25. Guyot-Sionnest, N. S., Villain, F., Bazin, D., Dexpert, H., Le Peltier, F., Lynch, J., and Bournonville, J. P., *Catal. Lett.* **8**, 283 (1991).
26. Barbier, J., *Appl. Catal.* **23**, 225 (1986).
27. Yang, O. B., Woo, S. I., and Hwang, I. C., *Catal. Lett.* **19**, 239 (1993).
28. Pieck, C. L., Marecot, P., Paveva, J. M., and Barbier, J., *Appl. Catal. A: General* **126**, 153 (1995).
29. Betramini, J. N., Wessel, T. J., and Datta, R., *AlChE* **37**(6), 845 (1991).
30. Querini, C. A., and Fung, S. C., *Appl. Catal. A: General* **117**, 53 (1994).
31. Steven, M. A., and Wolfgang, M. M. S., *J. Catal.* **116**, 184 (1989).
32. Jackson, S. D., Wills, J., McLellan, G. D., Webb, G., Keegan, M. B. T., Moyes, R. B., Simpson, S., Wells, P. B., and Whyman, R., *J. Catal.* **139**, 191 (1993).
33. Lieske, H., Lietz, G., Spindler, H., and Volter, J., *J. Catal.* **81**, 8 (1983).
34. Dautzenberg, F. H., and Wolters, H. B. M., *J. Catal.* **51**, 26 (1978).
35. Laiyuan, C., Yuequin, N., Jingling, Z., Liwu, L., Xihui, L., and Sen, S., *J. Catal.* **145**, 132 (1994).
36. Lee, T. J., and Kim, Y. G., *J. Catal.* **90**, 279 (1984).
37. Rios, G. A., Valenzuela, M. A., Armendariz, H., Salas, D., Dominguez, J. M., Acosta, D. R., and Schifter, I., *Appl. Catal. A: General* **90**, 25 (1992).
38. Rajeshwer, D., Basrur, A. G., Gokak, D. J., and Krisnamurthy, K. R., *J. Catal.* **150**, 135 (1994).
39. Mievile, R. L., *J. Catal.* **87**, 437 (1984).
40. Subramanian, S., and Schwarz, J. A., *Appl. Catal.* **68**, 131 (1991).
41. Mansour, A. N., Cook, J. W., Jr., Sayers, D. E., Emrich, R. J., and Katzer, J. R., *J. Catal.* **89**, 462 (1984).
42. Kobayashi, K., Yoshiki, M., Yagi, S., Kaneyuki, K., Yokoyama, T., Inokuchi, M., Tajima, H., Kitajima, Y., and Ohta, T., Photon Factory Activity Report 234, 1993.
43. Weiss, A. H., Valinski, S., and Antoshin, G. V., *J. Catal.* **74**, 136 (1982).
44. Zhou, X. L., and White, J. M., *Surf. Sci.* **185**, 450 (1987).
45. Kiskinova, M., and Goodman, D. W., *Surf. Sci.* **108**, 64 (1981).
46. Rasko, J., Bentovics, J., and Solymosi, F., *J. Catal.* **143**, 138 (1993).
47. Moulder, J. F., Stickle, W. F., Sobol, P. E., and Bomben, K. D., "Handbook of X-ray Photoelectron Spectroscopy," Perkin-Elmer Corp., Minnesota, 1992.